Highly Efficient Multi-resolution Topology Optimization Based on the Kriging-Interpolation Network

Wenliang Qian[1,2] and Hui Li[1,2(✉)]

[1] School of Civil Engineering, Harbin Institute of Technology, Harbin, China
lihui@hit.edu.cn

[2] Key Lab of Smart Prevention and Mitigation of Civil Engineering Disaster of the Ministry of Industry and Information Technology, Beijing, China

Abstract. Topology optimization aims to search for the optimal material distribution with a prescribed volume fraction. Recently, to reduce the computational cost of finite element analysis, multi-resolution topology optimization (MTOP) has been proposed to decouple the finite elements and density elements. However, MTOP introduces new problems with checkerboard patterns and numerous design variables, which hinder its popularity. To overcome these problems of MTOP and significantly improve the computational efficiency, an efficient multi-resolution topology optimization method based on the Kriging-Interpolation network (MTOP-KIN) is proposed in this paper. In the proposed MTOP-KIN, a customized single-layer neural network (Kriging-Interpolation network) is designed to express the topology description function of the design domain, avoiding the checkerboard patterns without filtering techniques or higher-order elements and reducing the design space. Several two-dimensional and three-dimensional numerical examples of topology optimization problems with compliance minimization are studied to demonstrate the effectiveness of the proposed method. The results show that the proposed MTOP-KIN can obtain better optimization results than MTOP. Meanwhile, compared with MTOP, an acceleration of about 11 to 18 times can be achieved.

Keywords: Multi-resolution topology optimization · Kriging-Interpolation network · Knot mesh · Topology description function

1 Introduction

To obtain the optimum structural performance, researchers have shown an increased interest in topology optimization since the pioneering work [1]. The goal of topology optimization is to find the optimal material distribution with the prescribed volume fraction to minimize the objective [2–4]. However, topology optimization is still not popular in the engineering field, especially for large-scale problems, due to the need for high computational resources.

D. Pavlou et al. (Eds.): OES 2023, SI 29, pp. 124–142, 2024.
https://doi.org/10.1007/978-3-031-49791-9_9

To overcome this computational burden, a series of works have been done to reduce computational cost or improve computational efficiency by saving the computational costs of updating the design variables or calculating the governing equations. In terms of design variables, Guest et al. [5] proposed a decoupling strategy to separate the design variable and the analysis mesh by the Heaviside projection method. Kim et al. proposed the reducible design variable method (RDVM) to save the computational costs of updating design variables by not considering the design variables that have converged [6]. In terms of solving the governing equations, iterative solvers, for example, a multigrid preconditioned conjugate gradients (MGCG) solver, are adopted to fast solve large-scale 3-D structural topology optimization problems on a standard PC [7, 8]. Another approach is to use a multiresolution topology optimization (MTOP) scheme to obtain high resolution designs by using a coarser discretization for finite elements and finer discretization for both density elements and design variables [9], which is a universal topology optimization method. According to this approach, finite element analysis will be performed in a relatively coarse mesh, which will significantly save time in solving the governing equations. However, MTOP has two disadvantages: the QR-patterns and numerous design variables. The QR-patterns means that the optimization results by this method consisted of artificially stiff regions named the QR-patterns as shown in Fig. 1, which seriously hurts the application of MTOP. The QR-patterns arise mainly due to the discontinuity of the density distribution in the element leading to the inability of the low-order shape functions to accurately model its displacement. To conquer this problem, several methods have been proposed, including the use of filtering (density projection) and the use of higher polynomial shape functions. When using the filtering in MTOP, the density field will be smoothed equivalent to imposing a restriction on minimum feature size. However, the filter radius is not easy to determine an appropriate value, where the large filter radius will restrict the design field from expressing a high order material distribution [10]. Meanwhile, the additional computational costs of computing filter weights and performing convolution operations are also an obstacle, especially on large scale problems. When using the higher polynomial elements in MTOP, the QR-patterns can be avoided in the simplest way by accurately modeling the displacement field [10–12]. But, the use of high order elements will increase the degrees of freedom so as to take more time to solve the governing equation, which contradicts the original purpose of MTOP. Another drawback, i.e. numerous design variables, arises from the introduction of the density mesh in MTOP. To overcome this problem, an adaptive isosurface variable grouping (aIVG) is proposed to group design variables of similar grouping criteria into a single grouped design variable [13], which will significantly reduce computation time in optimization.

In recent years, deep learning has made successive breakthroughs in several fields due to its powerful non-linear representation and efficient optimization algorithm [14–16]. Therefore, for the sake of completeness, it is also necessary to mention that several machine learning-based studies for topology optimization have been proposed. For example, a deep learning-based method is proposed to predict an optimized structure by designing convolutional neural networks to model the relationship between the optimization results and some parameters of the optimal topologies [17]. A novel two-phase methodology based on deep learning also is proposed to find the relationship between

the final density values of each finite element and the results of the first few iterations of the SIMP method [18]. Some reparameterization methods based on deep learning also be studied, where the design variables are the parameters of the network [19–21].

Since the above studies based deep learning either face generalizability problems, or interpretability problems, or computational efficiency problems, a general and efficient topology optimization method is worth investigating. As mentioned above, MTOP is a universal topology optimization method, and significantly save time in solving the governing equations. However, the QR-patterns and numerous design variables will lose the computational advantage of MTOP, preventing the further popularity of MTOP. So, once these problems can be overcome, MTOP will be the most promising approach to help topology optimization become popular in the engineering field.

Motivated by the aforementioned problems, this study aims to provide a novel method to avoid the QR-patterns and reduce the number of design variables without losing the computational advantage of MTOP. As is well-known, level set methods can avoid the checkerboard pattern, similar to the QR-patterns, without the filter technology. Topology description functions (TDF) based on the Kriging interpolation model [22, 23] are a class of explicit level-set methods to solve topology optimization, which can not only avoid the checkerboard phenomenon but also significantly reduce the number of design variables compared with element-wise density-based topology optimization. However, the methods based on the Kriging interpolation model are non-gradient methods and thus require high computational resources, since the gradient calculation is very difficult due to the fact that the material distribution is obtained by cutting the TDF with a certain threshold [23, 24]. Therefore, when the gradients can be easily calculated, the Kriging interpolation model will be a potential way to avoid the QR-patterns while reducing the number of design variables.

The remainder of this article is organized as follows. Section 2 describes the proposed multi-resolution topology optimization based on the Kriging-Interpolation network (MTOP-KIN) in detail. Section 3 conducts a series of 2D and 3D experiments to validate the proposed method and discusses the results. Section 4 presents a discussion about the effect of the Multiresolution Model on MTOP-KIN and the influence of the Knot mesh and Density mesh on MTOP-KIN. Section 5 summarizes and concludes the paper.

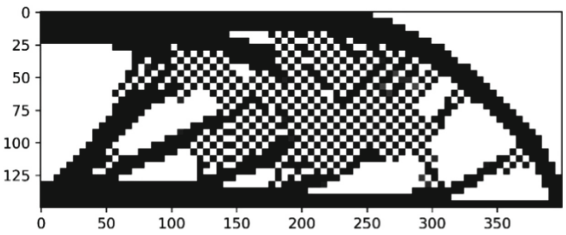

Fig. 1. The QR-patterns in optimization design obtained by MTOP

2 Method

A novel multi-resolution topology optimization using the Kriging-Interpolation network is proposed in this study, which is referred to as MTOP-KIN. The proposed MTOP-KIN can avoid QR patterns without filtering techniques or high-order elements and reduce the design space, thereby improving the computational efficiency for the topology optimization problems. It can divide into three parts: Multiresolution model, Physical model solver, and Model optimization, as shown in Fig. 2. The three parts of the proposed MTOP-KIN are described in detail in Sects. 2.1, 2.2, and 2.3 below, respectively.

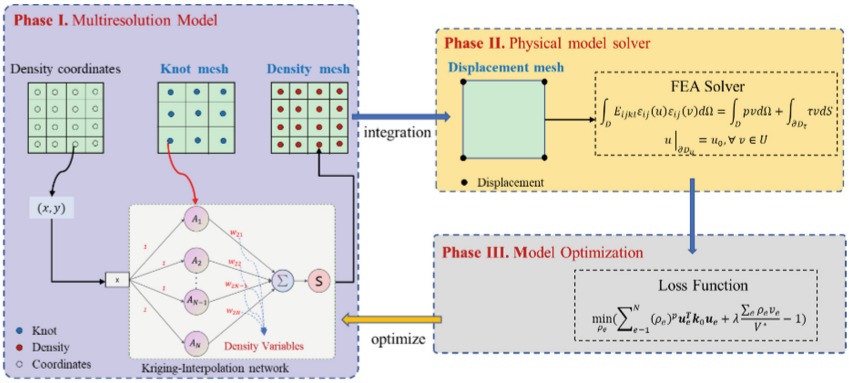

Fig. 2. The framework for the proposed multi-resolution topology optimization

2.1 Multiresolution Model

The goal of the Multiresolution model is to establish the relationship between the Knot mesh, Density mesh, and Displacement mesh, as shown in Fig. 3. By using these meshes, the Knot mesh to establish a topology description function, the Density mesh to determine density variables in the Displacement mesh, and Displacement mesh to perform finite element analysis can be decoupled from each other.

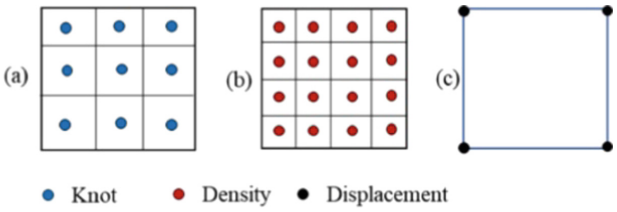

Fig. 3. The three different meshes for the multiresolution model: (a) Knot mesh, (b) Density mesh, (c) Displacement mesh

In the conventional MTOP, the design variable is equal to the number of density elements in Density mesh. But, in the MTOP-KIN, the number of design variables

is equal to the number of elements in the Knot mesh. Since the number of elements in the Knot mesh is usually smaller than the number of density variables in Density mesh, e.g. 9%, the Knot mesh can reduce the number of design variables than directly using the Density mesh. Also, as in conventional MTOP, the Displacement mesh can significantly reduce the time of solving the governing equation as the finite element analysis is performed in a relatively coarse mesh. For example, in Fig. 3, the number of elements in the Displacement mesh is only 6.25% of those in the Density mesh.

To avoid QR-patterns without losing the computational advantage of MTOP and reduce the design space, the Knot mesh adopts a Kriging-Interpolation method based a single-layer neural network to obtain density variables. Using this Kriging-Interpolation network, the topology description function (TDF) $f(x)$ is a combination of nonlinear activation function $A_i(x)$ in the hidden layer weighted by weights w_{ij} in the hidden layer. Then the $f(x)$ is acquired by the forward propagation of the network as follows

$$f(x) = \sum\nolimits_i w_{2i} A_i(w_{i0}x) = \sum\nolimits_i w_{2i} \mathrm{e}^{-\alpha^2 \|w_{i0}x - x_i\|^2} \tag{1}$$

Here, $A_i(w_{i0}x) = \mathrm{e}^{-\alpha^2 \|w_{i0}x - x_i\|^2}$ is the customized nonlinear activation function, $w_{i0} = 1$ and w_{2i} denote the corresponding weights of the single-layer neural network, x_i and α denote the center coordinates of elements in the Knot mesh and tuning constant, respectively. The α denotes the sharing degree between knots by

$$\alpha = \frac{1}{\tilde{r}} \sqrt{(ln(1/c)} \tag{2}$$

where $\tilde{r}$ is the minimum Euclidean distance between knots and c is a constant setting as 0.5 in this study. The learnable weights w_{2i}, i.e. design variables, will be updated by a backpropagation algorithm, where the number is equal to the numbers of elements in the Knot mesh. So, the number of design variables can be greatly reduced, which will improve the computational efficiency of MTOP. Meanwhile, since the only learnable weights w_{2i} represents the weights of different basis functions, this network is interpretable. The architecture of the proposed Kriging-Interpolation network is presented in Fig. 4, where the input is the center coordinates in the Density mesh and the output are the corresponding density values.

Here, the sigmoid activation function is adopted to convert the value $f(x)$ to a continuous density value $\rho(x) \in [0, 1]$ as:

$$\rho(x) = \frac{1}{1 + e^{-f(x)}} \tag{3}$$

This activation function will overcome the difficulty of calculating the gradient of the objective function with respect to the TDF by the cutting operation in the classical level-set method, where the aim of this cutting operation is to determine the material properties in the design domain by the relationship between the value $f(x)$ and the threshold value T_s as follows.

$$\begin{aligned} f(x) &\geq T_S, \quad \rho(x) = 1 \\ f(x) &< T_S, \quad \rho(x) = 0 \end{aligned} \tag{4}$$

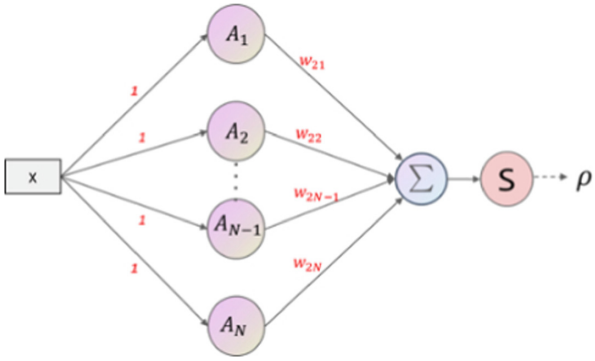

Fig. 4. The architecture of the proposed Kriging-Interpolation network

By using the proposed Kriging-Interpolation network, the density distribution in the density mesh will change smoothly, which can be observed in Fig. 5. The smaller the number of knots in the knot mesh, the smoother the change of density distribution in the Density mesh. Meanwhile, the values of density function $\rho(x)$ is a continuous function within the range of [0, 1] with convenience in the calculation of gradient, which also improves computational efficiency of MTOP by using gradient-based optimization methods, such as stochastic gradient descent (SGD), AdaGrad [25], and Adam [26].

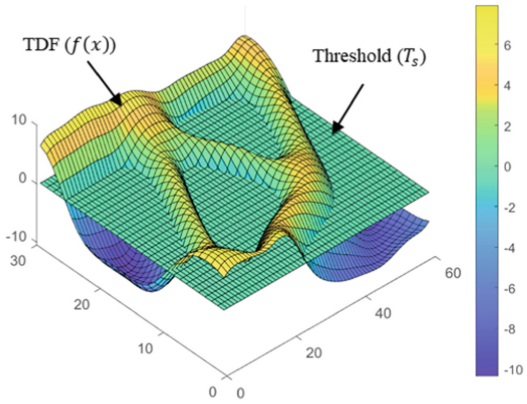

Fig. 5. The topology description function by the proposed Kriging-Interpolation network

2.2 Physical Model Solver

The goal of the Physical model solver is to solve the state field, involving the integration of the element stiffness matrix in the displacement mesh, material penalization model, and finite element analysis.

The integration of the element stiffness matrix is to compute the stiffness by considering the corresponding contribution of the density element over the displacement

element domain. Figure 6 presents the superposed meshes of the Density mesh and Displacement mesh, where a_i^e is the area or volume of the ith density element in the eth displacement element and ρ_i^e is the density value of the ith density element in the eth displacement element. Using the Gauss-Legendre quadrature, a modified displacement element stiffness can be expressed as

$$\boldsymbol{k^e} = \int_{\Omega^e} \mathbf{B^{eT}} \mathbf{C^e} \mathbf{B^e} \cong \sum_{i=1}^{N_n^e} \left(\mathbf{B^{eT}} \mathbf{C^e} \mathbf{B^e} \right)|_i a_i^e \tag{5}$$

where $\boldsymbol{k^e}$, Ω^e, $\mathbf{B^e}$, $\mathbf{C^e}$, and N_n^e is the element stiffness matrix, design domain, strain-displacement matrix, constitutive matrix, and number of density element of the eth displacement element, respectively.

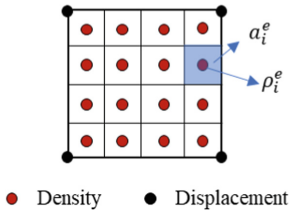

Fig. 6. The superposed meshes of the density mesh and displacement mesh

The material penalization model is to convert the integer optimization problem to a continuous optimization problem. In this study, the popular model named solid isotropic material with penalization (SIMP) is adopted [2]. And its formulation is $E_i(\rho_i) = \rho_i{}^p E_0$, where E_0 denotes the Young's modulus and p is the penalization factor, set to 3 in this study. Because the constitutive matrix depends on the modified Young's modulus of the material, the modified displacement element can be reexpressed by one value ρ_i^e as follows:

$$\boldsymbol{k^e} \cong \sum_{i=1}^{N_n} \left(\rho_i^e\right)^p \left(\mathbf{B^{eT}} \mathbf{C^e} \mathbf{B^e} \right)|_i a_i^e \tag{6}$$

The finite element analysis is to solve the state field, where the governing equation of the state field can be expressed by the energy bilinear form and the load linear form, and its formulation as

$$\int_D C_{ijkl} \varepsilon_{ij}(\boldsymbol{u}) \varepsilon_{ij}(\boldsymbol{v}) d\Omega = \int_D \boldsymbol{p} \boldsymbol{v} d\Omega + \int_{\partial D_\tau} \boldsymbol{\tau} \boldsymbol{v} dS \tag{7}$$

where C_{ijkl} is the fourth-order constitutive tensor, ε_{ij} is the linearized strains, $\boldsymbol{p}$ is the body forces, and $\boldsymbol{\tau}$ is the traction forces. By discretizing the design domain with displacement elements, i.e. the Displacement mesh, the governing equation can be formulated by the following discrete equations:

$$\mathbf{KU} = \mathbf{F} \tag{8}$$

where $\mathbf{U}$, $\mathbf{K}$ and $\mathbf{F}$ are the global displacement, stiffness matrix and force vectors, respectively. The $\mathbf{K}$ is obtained by assembling the element stiffness matrix $\boldsymbol{k^e}$, i.e. $\mathbf{K} = \sum_e \boldsymbol{k^e}$.

2.3 Model Optimization

The goal of the Model optimization is to search the optimal parameters of MTOP-KIN by optimizing the loss function, which aims at converting the constrained optimization problem of topology optimization into a network optimization by the Lagrange multiplier method. For the specific compliance minimization problems, the loss function can be written as follows:

$$L = \mathbf{U^T K U} + \lambda \left(\frac{V(\boldsymbol{\rho^e})}{V_0} - V_f^c \right)^2 \tag{9}$$

where λ., V_f^c, $V(\boldsymbol{\rho^e})$ and V_0 are Lagrangian penalty factor, the prescribed volume fraction, the material volume and volume of design domain, respectively. To control the order of magnitude of the different terms, the normalization is operated in Eq. (9), which is similar to that TOuNN in [19].

$$L = \frac{\mathbf{U^T K U}}{J_0} + \boldsymbol{\lambda} \left(\frac{V(\boldsymbol{\rho^e})}{V_0 \times V_f^c} - 1 \right)^2 \tag{10}$$

where J_0 is the objective function value of the randomly initialized MTOP-KIN before network training. In order to update the network parameters w_{2i}, the gradient can be calculated using the chain derivative rule as follows:

$$\frac{\partial L}{\partial \theta_{2i}} = \sum\nolimits_e \frac{\partial L}{\partial \rho^e} \frac{\partial \rho^e}{\partial f} \frac{\partial f}{\partial \theta_{2i}} \tag{11}$$

$$\frac{\partial L}{\partial \rho^e} = -\frac{1}{J_0} \left(\rho_j^e \right)^{p-1} \mathbf{u^{e^T}} \left(\mathbf{B^{e^T} C^e B^e} \right) |_j a_j^e \mathbf{u^e} + \frac{2\lambda}{V_f^c} \left(\frac{V(\rho^{\mathbf{e}})}{V_0 \times V_f^c} - 1 \right) \tag{12}$$

$$\frac{\partial \rho^{\mathbf{e}}}{\partial f} = \frac{e^{-f(x)}}{\left(1 + e^{-f(x)}\right)^2} \tag{13}$$

$$\frac{\partial f}{\partial w_{2i}} = e^{-\alpha^2 \|\mathbf{x} - x_i\|^2} \tag{14}$$

where Eqs. (13) and (14) can be obtained directly by the backpropagation algorithm. Adam [26] is one of the most popular optimization algorithms in deep learning due to its good performance. So, Adam is adopted to optimize the MTOP-KIN. In optimization, checking the convergence is also important, which can affect the computational efficiency of topology optimization. The change of the loss function in deep learning is often used to determine the convergence, so a natural idea is to use the change of the loss function as the convergence criterion for the proposed MTOP-KIN.

Here, the standard deviation of objective function values of successive iterations is adopted to determine the convergence status of MTOP-KIN as follows:

$$\overline{L}_i = \frac{L_{i-(NC-1)} + L_{i-(NC-2)} + \cdots + L_{i-1} + L_i}{NC} \tag{15}$$

$$\sigma_i = \sqrt{\frac{1}{NC-1}\sum_{j=i-(NC-1)}^{i}\left(L_j - \overline{L}_i\right)^2} \tag{16}$$

where NC denotes the number of successive iterations for checking the convergence status and $i \geq NC$. When the standard deviation σ_i is less than a convergence tolerance value $\widetilde{\sigma}$, the convergence is considered to be reached.

3 Numerical Experiments

To investigate the performance of the proposed MTOP-KIN four structures are employed as examples, including three 2D structures and one 3D structure. In all examples, the volume fraction, the density penalization power, Young's modulus, and Poisson's ratio are set as 0.5, 3, 1.0, and 0.3. For the convenience of the subsequent discussion, the ratio of the number of the Knot mesh elements to the number of the Density mesh elements and the ratio of the number of the Density mesh elements to the number of the Displacement mesh elements are defined as follows

$$R_1 = N_{knot}/N_{desity} \tag{17}$$

$$R_2 = N_{desity}/N_{displacement} \tag{18}$$

where N_{knot}, N_{desity}, and $N_{displacement}$ denote the number of elements in the Knot mesh, Density mesh, and Displacement mesh, respectively. In all four different examples below, the R_1 and R_2 are set as 0.3 and 5, respectively. The learning rate of Adam is set as 0.3 and coefficients used for computing running averages of gradient and its square are set as $\beta_1 = 0.5$ and $\beta_2 = 0.999$, respectively. The number of successive iterations and convergence tolerance value for convergence condition is set as 15 and 0.0005, respectively.

3.1 2D Examples

The design domains of all 2D examples are assumed to be discretized by using a mesh of 80×30 square finite elements (Q4 elements) in the Displacement mesh of MTOP-KIN and MTOP, where the Density mesh is 400×150 and the Knot mesh is 120×45. The design domains and boundary conditions are shown in Fig. 7. To verify the performance of the proposed MTOP-KIN method, MTOP is selected as a baseline [9] and the filter radius is 5. Figure 8 gives the convergence curves of MTOP-KIN, from which it can be seen that the convergence is achieved in about 80 iterations.

These curves also illustrate that MTOP-KIN can achieve convergence performance under the same parameters for different examples. The optimization results generated by the proposed MTOP-KIN and MTOP are shown in Fig. 9. As presented, MTOP-KIN allows for clearer results without the use of filter techniques, i.e. gray regions are much fewer to compare with MTOP. This phenomenon indicates the feasibility of MTOP-KIN. Meanwhile, the QR-patterns also did not appear in the optimization results, which illustrates that the proposed method can avoid this problem without filtering techniques or high-order elements.

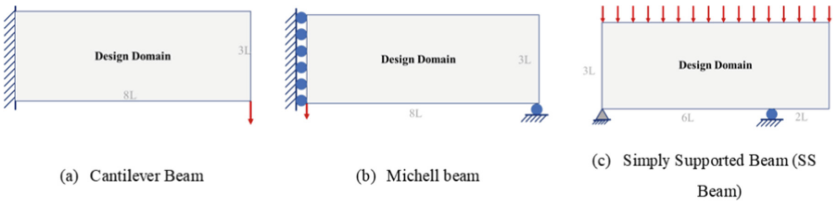

(a) Cantilever Beam (b) Michell beam (c) Simply Supported Beam (SS Beam)

Fig. 7. The design domains and boundary conditions of the cantilever beam, Michell beam and SS beam

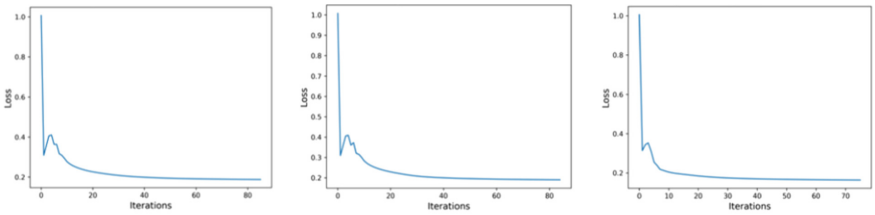

(a) Cantilever Beam (b) Michell beam (c) SS Beam

Fig. 8. The convergence curves of loss function in the training process on the cantilever beam, Michell beam and SS beam

Table 1 presents a summary of the proposed MTOP-KIN and MTOP, including the number of design variables, objective function values, and calculation time, on all test examples. These results show that the number of design variables of MTOP-KIN is much smaller than those of MTOP because the Knot mesh and nonlinear activation function $A_i(x)$ are adopted in MTOP-KIN. From these results, it can also be found that the compliance of the proposed method is smaller than that of MTOP, and a speedup of approximately 15 to 18 times is achieved compared with the MTOP method. The reason for the faster speed is mainly due to the reduction of design variables and the absence of filtering techniques.

3.2 3D Cantilever Beam

In this subsection, a 3D compliance minimization problem is also performed to verify that the proposed method can be applied not only to 2D but also to 3D. Figure 10 gives the 3D Cantilever Beam subjected to the unit loads. The design domain is discretized by using a mesh of $42 \times 12 \times 4$ cube finite elements in the Displacement mesh of MTOP-KIN and MTOP. Here, the Density mesh is $210 \times 60 \times 20$ and the Knot mesh is $63 \times 18 \times 6$. Using the MTOP-KIN, the convergence is achieved in about 70 iterations, as shown in Fig. 11. Figure 12 presents the optimization results by the MTOP-KIN and MTOP, indicating the proposed method is also suitable for 3D structures. From the optimization results, more thin members exist in the optimization result obtained by MTOP-KIN which means that better structures may be found by the proposed method. This can be verified by the compliance value, as listed in Table 2. The difference in the compliance value indicates that the stiffness of structure obtained by MTOP-KIN is much greater than the stiffness of that obtained by MTOP. Table 2 also shows that

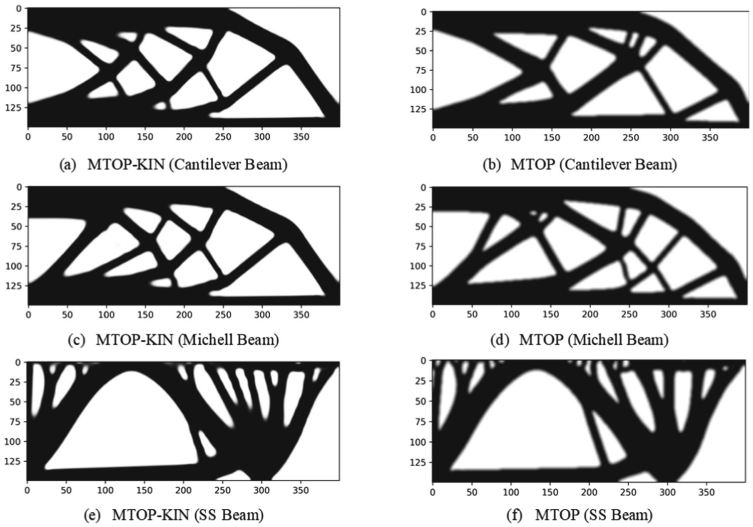

Fig. 9. Optimization results of the cantilever beam, Michell beam and simply supported (SS) beam

Table 1. Summary of the tested examples on the cantilever beam, Michell beam and simply supported (SS) beam

Case	Methods	No. of design variables	Obj. func. value	Time (s)
Cantilever beam	MTOP-KIN	**5400**	**134.88**	**5.08**
	MTOP	60000	140.51	80.99
Michell beam	MTOP-KIN	**5400**	**142.10**	**5.18**
	MTOP	60000	150.60	81.34
SS beam	MTOP-KIN	**5400**	**22605.42**	**4.20**
	MTOP	60000	23155.92	78.28

the proposed MTOP-KIN has a speedup of approximately 11 times compared with the MTOP method.

4 Discussions

The results of numerical experiments had illustrated the proposed MTOP-KIN can obtain better optimization results with less optimization time compared with MTOP, as outlined in Sect. 3. However, the key model and parameters still need to be investigated to explore their effect, for example, the effect of the multiresolution model and the influence of the number of knot elements and density elements on MTOP-KIN. So, first, the MTOP-KIN without the Multiresolution Model, named TOP-KIN, is investigated on the Cantilever Beam, Michell beam, and SS Beam. Then, the influence of the Knot mesh and Density

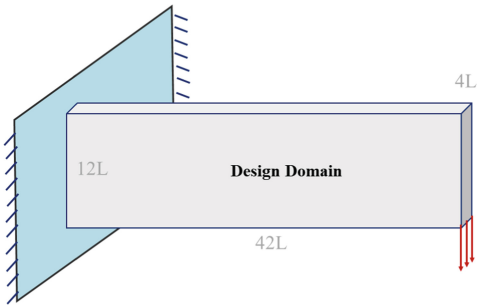

Fig. 10. The design domains and boundary conditions of the 3D cantilever beam

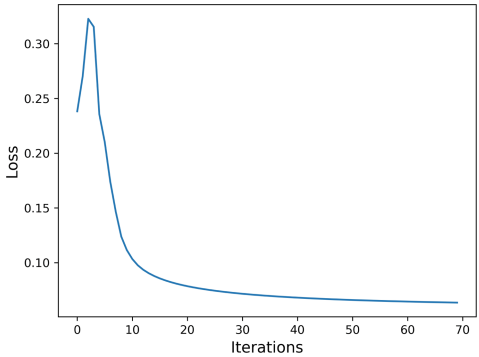

Fig. 11. The convergence curves of loss function in the training process on the 3D cantilever beam

Table 2. Summary of the tested examples on the 3D cantilever beam

Case	Methods	No. of design variables	Obj. func. value	Time (s)
3D cantilever beam	MTOP-KIN	**6804**	**2703.69**	**35.59**
	MTOP	252000	3742.08	396.75

mesh on MTOP-KIN is investigated on the SS Beam. Because the optimization result of the SS Beam has more members, the change of the optimized structure can be easily observed.

4.1 Effect of the Multiresolution Model on MTOP-KIN

The proposed MTOP-KIN comprises three parts: Multiresolution Model, Physical model solver, and Model optimization, as shown in Fig. 1. The most important part is Multiresolution Model to model the relationship between the Knot mesh, Density mesh, and Displacement mesh, where the Density mesh is the bridge that connects Knot mesh and

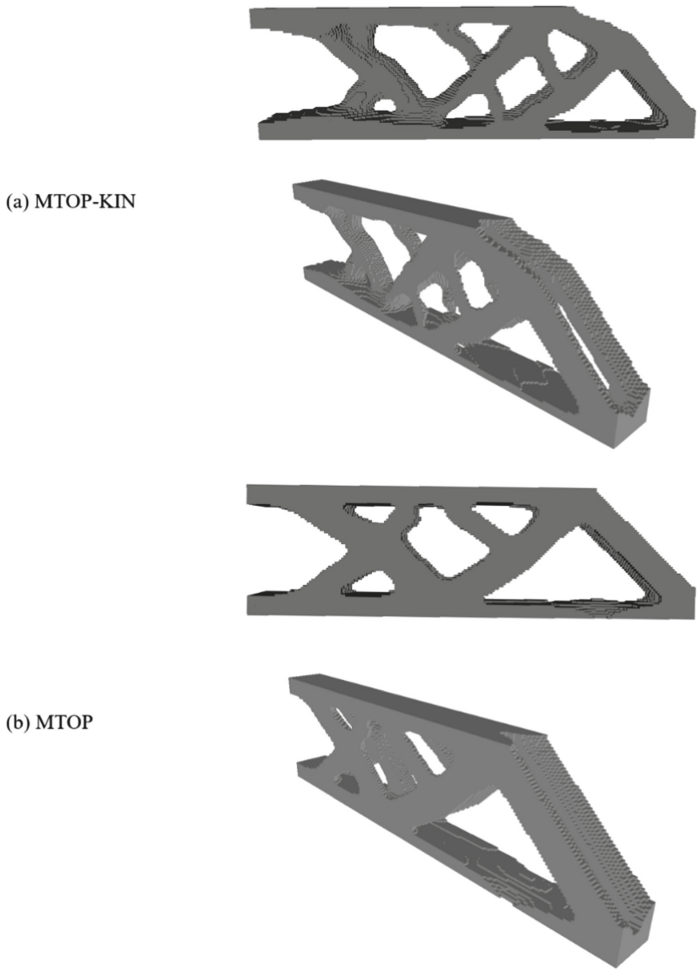

Fig. 12. Optimization results of the cantilever beam, Michell beam and simply supported (SS) beam

Displacement mesh. So, only using the Knot mesh and Displacement mesh in MTOP-KIN will be able to explain the role of the Multiresolution Model, this modified topology optimization method is called TOP-KIN.

Here, the number of elements in the Knot mesh and Displacement mesh of TOP-KIN is 120×45 and 80×30, which equal to those of MTOP-KIN, as described in Sect. 3.1. Figure 13 and Table 3 give the optimization results and the performance comparisons, respectively. From the results of Fig. 13, it can be found that MTOP-KIN can obtain a clearer optimization result with a higher resolution which means more thin members appear in the result. Table 3 shows that the optimization results have a much lower compliance value and the training time is only about twice that of the TOP-KIN.

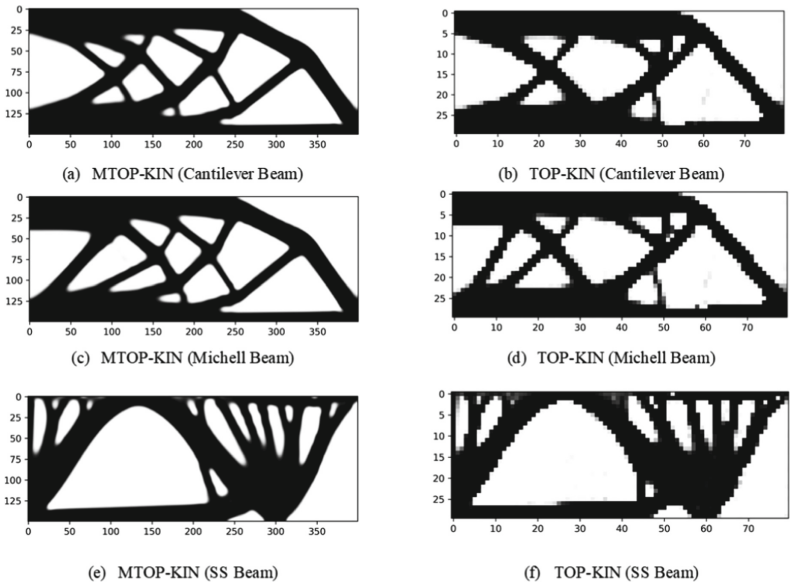

Fig. 13. Optimization results of the cantilever beam, Michell beam, and SS beam by MTOP-KIN and TOP-KIN

Table 3. Summary of the tested examples with MTOP-KIN and TOP-KIN

Case	Methods	No. of design variables	Obj. func. value	Time (s)
Cantilever beam	MTOP-KIN	5400	**134.88**	5.08
	TOP-KIN	5400	142.37	**2.39**
Michell beam	MTOP-KIN	5400	**142.10**	5.18
	TOP-KIN	5400	148.98	**2.51**
SS beam	MTOP-KIN	5400	**22605.42**	4.20
	TOP-KIN	5400	23122.41	**2.20**

Although the training time of MTOP-KIN increases compared with TOP-KIN, the TOP-KIN will consume more time to achieve the same resolution compared with the proposed MTOP-KIN. To illustrate this phenomenon, the Knot mesh and Displacement mesh in TOP-KIN are adjusted to 120×45 and 400×150, where the aim here is to make the number of elements in the Displacement mesh of TOP-KIN equal to the number of elements in the Density mesh of MTOP-KIN for obtaining the same resolution. For ease of description, the TOP-KIN of this configuration is noted as TOP-KIN-5. Figure 14 illustrates the MTOP-KIN can get almost the same optimization results with less Displacement mesh, meaning the optimization time can be significantly reduced. Meanwhile, Fig. 14(e) and (f) also clearly illustrate that MTOP-KIN gives better optimization results. These conclusions can be verified by the results in Table 4, which shows that

MTOP-KIN can not only get a much lower compliance value but also achieve a speedup of approximately 11 times.

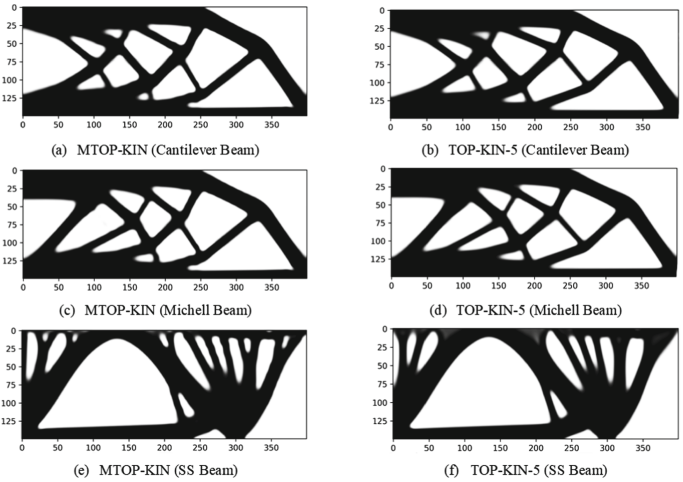

Fig. 14. Optimization results of the cantilever beam, Michell beam and SS beam by MTOP-KIN and TOP-KIN-5

Table 4. Summary of the tested examples with MTOP-KIN and TOP-KIN-5

Case	Methods	No. of design variables	Obj. func. value	Time (s)
Cantilever beam	MTOP-KIN	5400	**134.88**	**5.08**
	TOP-KIN-5	5400	138.93	60.72
Michell beam	MTOP-KIN	5400	**142.10**	**5.18**
	TOP-KIN-5	5400	148.41	59.05
SS beam	MTOP-KIN	5400	**22605.42**	**4.20**
	TOP-KIN-5	5400	22788.34	51.90

4.2 Effect of the Knot Mesh and Density Mesh on MTOP-KIN

The Knot mesh can control the degree of smoothing of the change of density distribution in the Density mesh, and the Density mesh controls the stiffness of the element in the Displacement mesh. Therefore, it is necessary to investigate the effect of the Knot mesh and Density mesh on MTOP-KIN.

The influence of the Knot mesh is first investigated. In order to exclude the effect of the Displacement and Density meshes, the number of elements remains the same, and only the number of the Knot mesh is changed. Eight different Knot mesh configurations were investigated with the ratio of the number of elements of the Knot mesh and Density

mesh are 0.20, 0.25, 0.30, 0.35, 0.37, 0.39, 0.40, and 0.41, respectively. Figure 15 and Table 5 give the optimization results and performance comparisons. These results show that the resolution of the structure becomes higher and objective function values come to be smaller, as the number of elements in the Knot mesh increases. But, the degree of smoothing of the optimization results obtained by MTOP-KIN with $R_1 = 0.40$ and $R_1 = 0.41$ are worse than the results of the other configurations.

Then the influence of the Density mesh is investigated. Similarly, only the ratio of the number of the density mesh elements to the number of the displacement mesh elements is changed with the same Displacement mesh and $R_1 = 0.30$. Six different ratios R_2 were investigated are 2, 3, 4, 5, 6 and 7. From the results of Fig. 16 and Table 5, it can be observed that structures with isolated islands will occur when unsuitable R_2 is adopted. Because the more the number of knots in the Knot mesh means that $\alpha = \frac{1}{r}\sqrt{(ln(1/c)}$ is smaller, the smoothing effect on the Density mesh will decrease, leading to drastic changes or even discontinuity of density in the Density mesh. Fortunately, through the extensive experiments, including 2D and 3D experiments, it can be found that a suitable ratio of elements of the Knot mesh and Displacement mesh should satisfy $R_1 \times R_2 \in [1.3, 1.8]$, which can help the proposed MTOP-KIN generate clear and smooth optimization results (Table 6).

Table 5. Summary of the SS beam by MTOP-KIN with different knot meshes

R_1	Obj. func. value	R_1	Obj. func. value
0.20	23004.08	0.37	22436.90
0.25	22787.96	0.39	22396.11
0.30	22605.42	0.40	22391.78
0.35	22502.78	0.41	22338.00

Table 6. Summary of the SS beam by MTOP-KIN with different density meshes

R_2	Obj. func. value	R_2	Obj. func. value
2	23588.38	5	22605.42
3	23113.61	6	22449.35
4	22812.90	7	22324.90

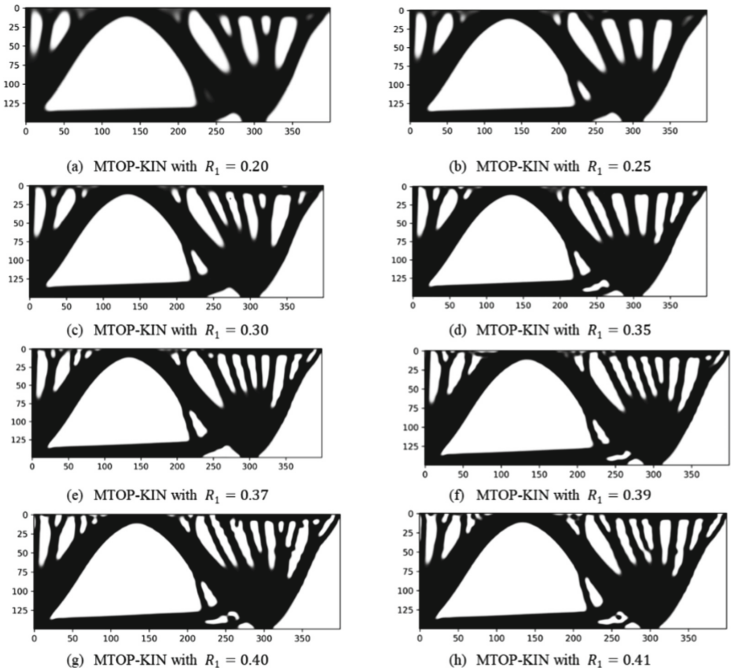

(a) MTOP-KIN with $R_1 = 0.20$ (b) MTOP-KIN with $R_1 = 0.25$

(c) MTOP-KIN with $R_1 = 0.30$ (d) MTOP-KIN with $R_1 = 0.35$

(e) MTOP-KIN with $R_1 = 0.37$ (f) MTOP-KIN with $R_1 = 0.39$

(g) MTOP-KIN with $R_1 = 0.40$ (h) MTOP-KIN with $R_1 = 0.41$

Fig. 15. Optimization results of the SS beam by MTOP-KIN with different knot meshes

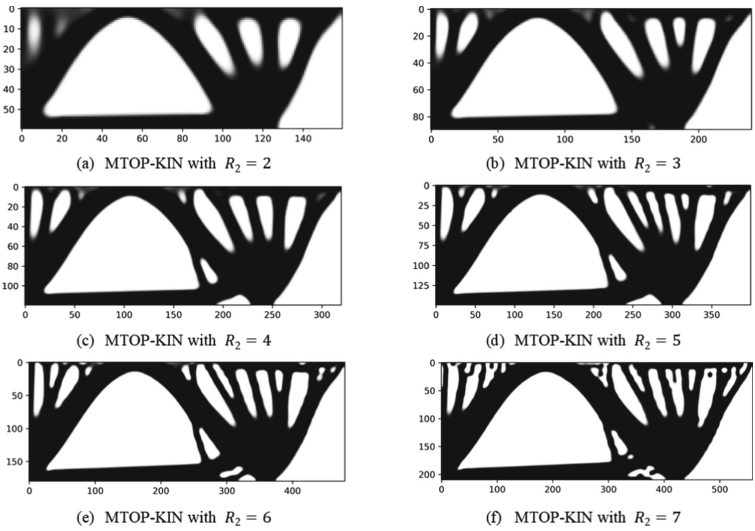

(a) MTOP-KIN with $R_2 = 2$ (b) MTOP-KIN with $R_2 = 3$

(c) MTOP-KIN with $R_2 = 4$ (d) MTOP-KIN with $R_2 = 5$

(e) MTOP-KIN with $R_2 = 6$ (f) MTOP-KIN with $R_2 = 7$

Fig. 16. Optimization results of the SS beam by MTOP-KIN with different density meshes

5 Conclusion

This paper proposes a novel multi-resolution topology optimization based on the Kriging-Interpolation network using a customized single-layer neural network to express the topology description function of a design domain. The proposed can obtain better optimization results using less time compared with MTOP.

The main conclusions are summarized as follows:

- The MTOP-KIN can avoid QR patterns without filtering techniques or high-order elements by the proposed Kriging-Interpolation network to model the relationship between the Knot elements and Density elements, which maintains the computational advantage of multi-resolution topology optimization.
- The proposed Kriging-Interpolation network in MTOP-KIN is interpretable since all parameters in this network are straightforward linked with those in topology description function and have a clear physical sense. Meanwhile, with this network, the design variables of MTOP-KIN can be updated by gradient-based optimization algorithms and GPU.
- The proposed MTOP-KIN can reduce the design space by a novel topology description function and obtain a better optimization result with a speedup of approximately 11 to 18 times compared with the MTOP method for 2D and 3D examples.

Acknowledgement. This study is financially supported by National Natural Science Foundation of China No. 51921006.

References

1. Bendsøe, Martin P. "Optimal shape design as a material distribution problem." *Structural optimization* 1 (1989): 193–202.
2. Bendsøe, Martin P., and Ole Sigmund. "Material interpolation schemes in topology optimization." *Archive of applied mechanics* 69 (1999): 635–654.
3. Xie, Yi Min, and Grant P. Steven. "A simple evolutionary procedure for structural optimization." *Computers & structures* 49.5 (1993): 885–896.
4. Yulin, Mei, and Wang Xiaoming. "A level set method for structural topology optimization and its applications." *Advances in Engineering software* 35.7 (2004): 415–441.
5. Guest, James K., and Lindsey C. Smith Genut. "Reducing dimensionality in topology optimization using adaptive design variable fields." *International journal for numerical methods in engineering* 81.8 (2010): 1019–1045.
6. Kim, Sun Yong, Il Yong Kim, and Chris K. Mechefske. "A new efficient convergence criterion for reducing computational expense in topology optimization: reducible design variable method." *International journal for numerical methods in engineering* 90.6 (2012): 752–783.
7. Amir, Oded, Niels Aage, and Boyan S. Lazarov. "On multigrid-CG for efficient topology optimization." *Structural and Multidisciplinary Optimization* 49 (2014): 815–829.
8. Peetz, Darin, and Ahmed Elbanna. "On the use of multigrid preconditioners for topology optimization." *Structural and Multidisciplinary Optimization* 63 (2021): 835–853.
9. Nguyen, Tam H., et al. "A computational paradigm for multiresolution topology optimization (MTOP)." *Structural and Multidisciplinary Optimization* 41 (2010): 525–539.

10. Gupta, Deepak K., Matthijs Langelaar, and Fred van Keulen. "QR-patterns: artefacts in multiresolution topology optimization." *Structural and Multidisciplinary Optimization* 58 (2018): 1335–1350.
11. Groen, Jeroen P., et al. "Higher-order multi-resolution topology optimization using the finite cell method." *International Journal for Numerical Methods in Engineering* 110.10 (2017): 903–920.
12. Nguyen, Tam H., Chau H. Le, and Jerome F. Hajjar. "Topology optimization using the p-version of the finite element method." *Structural and Multidisciplinary Optimization* 56 (2017): 571–586.
13. Yoo, Jaeeun, In Gwun Jang, and Ikjin Lee. "Multi-resolution topology optimization using adaptive isosurface variable grouping (MTOP-aIVG) for enhanced computational efficiency." *Structural and Multidisciplinary Optimization* 63 (2021): 1743–1766.
14. Davies, Alex, et al. "Advancing mathematics by guiding human intuition with AI." *Nature* 600.7887 (2021): 70–74.
15. Silver, David, et al. "Mastering the game of go without human knowledge." *nature* 550.7676 (2017): 354–359.
16. Tunyasuvunakool, Kathryn, et al. "Highly accurate protein structure prediction for the human proteome." *Nature* 596.7873 (2021): 590–596.
17. Yu, Yonggyun, et al. "Deep learning for determining a near-optimal topological design without any iteration." *Structural and Multidisciplinary Optimization* 59.3 (2019): 787–799.
18. Kallioras, Nikos Ath, Georgios Kazakis, and Nikos D. Lagaros. "Accelerated topology optimization by means of deep learning." *Structural and Multidisciplinary Optimization* 62.3 (2020): 1185–1212.
19. Chandrasekhar, Aaditya, and Krishnan Suresh. "TOuNN: Topology optimization using neural networks." *Structural and Multidisciplinary Optimization* 63 (2021): 1135–1149.
20. Deng, Hao, and Albert C. To. "A parametric level set method for topology optimization based on deep neural network." *Journal of Mechanical Design* 143.9 (2021): 091702
21. Zhang, Zeyu, et al. "TONR: An exploration for a novel way combining neural network with topology optimization." *Computer Methods in Applied Mechanics and Engineering* 386 (2021): 114083.
22. Hamza, Karim, Mohamed Aly, and Hesham Hegazi. "A kriging-interpolated level-set approach for structural topology optimization." *Journal of Mechanical Design* 136.1 (2014): 011008.
23. Guirguis, David, William W. Melek, and Mohamed F. Aly. "High-resolution non-gradient topology optimization." *Journal of Computational Physics* 372 (2018): 107–125.
24. Guirguis, David, and Mohamed F. Aly. "A derivative-free level-set method for topology optimization." *Finite Elements in Analysis and Design* 120 (2016): 41–56.
25. Duchi, John, Elad Hazan, and Yoram Singer. "Adaptive subgradient methods for online learning and stochastic optimization." *Journal of machine learning research* 12.7 (2011).
26. Kingma, Diederik P., and Jimmy Ba. "Adam: A method for stochastic optimization." *arXiv preprint* arXiv:1412.6980 (2014).